Journal of Computational Applied Mechanics 2025, 56(2): 457-469

DOI: 10.22059/jcamech.2025.390562.1370

RESEARCH PAPER

Exact solutions for Two-dimensional flow of Fractional NTNN fluid within an oscillatory rectangular enclosure

Sohail Nadeem [a, b, c, *], Sobia Naz [a], Bushra Ishtiaq [a], Jehad Alzabut [b, d]

[a] *Department of Mathematics, Quaid-I-Azam University 45320, Islamabad 44000, Pakistan*
[b] *Department of Mathematics and Sciences, Prince Sultan University, 11586, Riyadh, Saudi Arabia*
[c] *Department of Mathematics, Wenzhou University, Wenzhou, 325035, China*
[d] *Department of Industrial Engineering, OSTIM Technical University, Ankara 06374, Türkiye*

Abstract

In this paper, we present an analysis for the unsteady two-dimensional flow of incompressible fractional NTNN model. The purpose of this research is to detect exact solutions for the cosine oscillation inside an oscillating rectangular duct having fractional fluid. The mixed initial-boundary value problem is simplified by using Laplace and double finite Fourier sine transform. The impacts of pertinent parameters on the velocity profile and the corresponding shear stresses are analysed through graphical illustrations for cosine oscillation. Our results indicate that the fluid's flow rises in correlation with fractional and rheological factors, such as α, N, ω, and t. As limiting cases of exact solution, the results can also be obtained for the ordinary NTNN and Newtonian fluid.

Keywords: Fractional calculus, Fractional Nadeem trigonometric non-Newtonian Model, Non-Newtonian fluid, Oscillating rectangular duct.

1. Introduction

Fractional calculus, the study of derivatives and integrals with non-integer orders, boasts a historical lineage nearly as rich as that of classical calculus with integer orders. This concept emerged nearly concurrently with classical calculus, tracing back to a notable exchange between G. W. Leibniz and L'Hospital (1695), where they pondered a significance of half derivatives. The FC theory more like an extension of the ordinary derivatives and due to its far-ranging applications in many fields of science and engineering it has gained the much need attention [1]. In the 19th century and onward, fractional calculus has gained significant momentum and present itself as a cornerstone for applied field such as factional geometry, fractional dynamics, and fractional differential equations. The practicality of fractional calculus is endless with endless applications in modern mathematics such as mechatronics, signal and image processing, environmental science. It even has application in the medical field. It can be applicable in tuberculosis and Ebola treatment [2, 3]. Aguilar et al. [4] did a study and analysis which was aimed at exploring the practicality of FC theory together with artificial neural networks (ANNs). Their research was aimed towards a comprehensive oversight over the key characteristics and application of ANNs backed by enhanced fractional calculus theory. On the other hand, Sheikh et al. [5] worked on the transfer of heat and mass within unstable Magnetohydrodynamic (MHD) fluids flow in Casson fluid within a vertical channel. They put to concept of Caputo time fractional derivative along with Fick's and Fourier's law to work in order to conduct their investigation. Sene [6] shed light on the discussion that by utilizing Caputo derivative along with finding their exact solution using

* Corresponding author: *Email Address:* sohail@qau.edu.pk

Laplace transform and Fourier sine transform. Nadeem et al [7] discussed the analysis of fractional derivative applied to a hybrid nanofluid of brinkman type which was aimed at exploring the implications of inclined magnetic field. Rauf et al. [8] delve into the study of unsteady multilayer laminar flow of incompatible factional second grade fluid that are confined in between a rectangular channel made by two parallel plates.

Non-Newtonian fluids have a lot of applications in engineering and industries. Among some of those applications are gels, lubricants, sprays and much more. The hardest thing in this fluid mechanics is predicting the behavior of non- Newtonian fluids. There are many research that are being done to understand the behavior of non-Newtonian fluids. The fractional NTNN is a non-Newtonian which was discussed by Nadeem et al [9]. The analysis of authors focused on applying the Caputo fractional derivative to examine the unsteady flow of a non-Newtonian fluid depicted by a trigonometric type. Barmak et al. [10] evaluated analytical solution of the steady laminar flow of a non-Newtonian fluid in a rectangular duct. Nadeem et al. [11] were identifying the analytical solution of squeezing flow of trigonometric non-Newtonian fluid between two infinite parallel heated plates with the help of differential transform method. Analytical solution of the unsteady rotational flow through an infinite circular cylinder of a non-Newtonian fluids with fractional-order derivative was obtained by Ghalib et al. [12]. The most recent research on fractional-order non-Newtonian fluids is described in [13-16].

The purpose of this paper is to study the two-dimensional unsteady flow of fractional NTNN fluid through an oscillating rectangular duct. The focus of this research is on the cosine oscillation of a rectangular cross-section duct. The exact solution for the field of velocity and shear stress is obtained by using the double finite Fourier sine transform and the discrete Laplace transform. Notably, regular NTNN and Newtonian fluid are studied as special cases. This analysis is prominent for its originality because no one has explored it before. Lastly, the impacts of some rheological factors and fractional order factors on the flow of fluid are represented graphically.

2. Nadeem trigonometric non-Newtonian model (NTNN)

The equation for an incompressible fractional NTNN model is given as

$$\boldsymbol{T} = -p\boldsymbol{I} + \boldsymbol{S}.$$

Here $\boldsymbol{T}$ is Cauchy stress, $p\boldsymbol{I}$ is the indeterminate spherical stress, and $\boldsymbol{S}$ is extra stress tensor which is define as

$$\boldsymbol{S} = \mu \boldsymbol{A_1} + \frac{1}{\theta_1 \gamma} sinh^{-1}\left(\frac{\gamma}{\theta_2}\right)\boldsymbol{A_1}. \tag{1}$$

where $\boldsymbol{A_1} = \boldsymbol{L} + (\boldsymbol{L})^T$.

After the first order expansion of $sinh^{-1}\left(\frac{\gamma}{\theta_2}\right) \approx \frac{\gamma}{\theta_2}$, Eq. (1.5) becomes

$$\boldsymbol{S} = \mu A_1 + \frac{1}{\theta_1 \theta_2} \boldsymbol{A_1}. \tag{2}$$

We can also be used $sin\left(\frac{\gamma}{\theta_2}\right), tan\left(\frac{\gamma}{\theta_2}\right), sin^{-1}\left(\frac{\gamma}{\theta_2}\right), tan^{-1}\left(\frac{\gamma}{\theta_2}\right), sinh\left(\frac{\gamma}{\theta_2}\right), tanh\left(\frac{\gamma}{\theta_2}\right)$, and $tanh^{-1}\left(\frac{\gamma}{\theta_2}\right)$ instead of using $sinh^{-1}\left(\frac{\gamma}{\theta_2}\right)$ in Eq. (1). By utilizing these trigonometric functions, the stress tensor is expressed like this below

$$\begin{aligned}
\boldsymbol{S} &= \mu A_1 + \frac{1}{\theta_1 \gamma} sin\left(\frac{\gamma}{\theta_2}\right)\boldsymbol{A_1},\\
\boldsymbol{S} &= \mu A_1 + \frac{1}{\theta_1 \gamma} tan\left(\frac{\gamma}{\theta_2}\right)\boldsymbol{A_1},\\
\boldsymbol{S} &= \mu A_1 + \frac{1}{\theta_1 \gamma} sin^{-1}\left(\frac{\gamma}{\theta_2}\right)\boldsymbol{A_1},\\
\boldsymbol{S} &= \mu A_1 + \frac{1}{\theta_1 \gamma} tan^{-1}\left(\frac{\gamma}{\theta_2}\right)\boldsymbol{A_1},\\
\boldsymbol{S} &= \mu A_1 + \frac{1}{\theta_1 \gamma} sinh\left(\frac{\gamma}{\theta_2}\right)\boldsymbol{A_1},\\
\boldsymbol{S} &= \mu A_1 + \frac{1}{\theta_1 \gamma} tanh\left(\frac{\gamma}{\theta_2}\right)\boldsymbol{A_1},
\end{aligned} \tag{3}$$

$$\boldsymbol{S} = \mu A_1 + \frac{1}{\theta_1 \gamma} tanh^{-1}\left(\frac{\gamma}{\theta_2}\right)\boldsymbol{A_1}.$$

The first-order expansion to the previously mentioned trigonometric type functions is applied and here is what we have obtained.

$$\begin{aligned} &sin\left(\frac{\gamma}{\theta_2}\right) \approx \frac{\gamma}{\theta_2},\\ &tan\left(\frac{\gamma}{\theta_2}\right) \approx \frac{\gamma}{\theta_2},\\ &sin^{-1}\left(\frac{\gamma}{\theta_2}\right) \approx \frac{\gamma}{\theta_2},\\ &sinh\left(\frac{\gamma}{\theta_2}\right) \approx \frac{\gamma}{\theta_2},\\ &tanh\left(\frac{\gamma}{\theta_2}\right) \approx \frac{\gamma}{\theta_2},\\ &tanh^{-1}\left(\frac{\gamma}{\theta_2}\right) \approx \frac{\gamma}{\theta_2}. \end{aligned} \tag{4}$$

The extra stress tensor expressions given in Eq. (3) are resulting in single equation after using Eq. (4) in Eq. (3).

$$\boldsymbol{S} = \mu \boldsymbol{A_1} + \frac{1}{\theta_1 \theta_2} \boldsymbol{A_1}. \tag{5}$$

Where $\boldsymbol{A_1} = \boldsymbol{L} + (\boldsymbol{L})^T$. Here $\boldsymbol{L}$ represents the velocity gradient and $\boldsymbol{L}^T$ denotes the transpose of the velocity gradient.

3. Problem formulation

Consider an incompressible fractional NTNN fluid within a rectangular duct, bounded by $x = 0$ to $x = d$ and $y = 0$ to $y = h$ as depicted in Fig.1. Initially, the duct is stationary, but on time $t = 0^+$, it begins to oscillate on the $z - axis$. The field of velocity is illustrated as $v\ (x, y, z) = w\ (x, y, t) = w$.

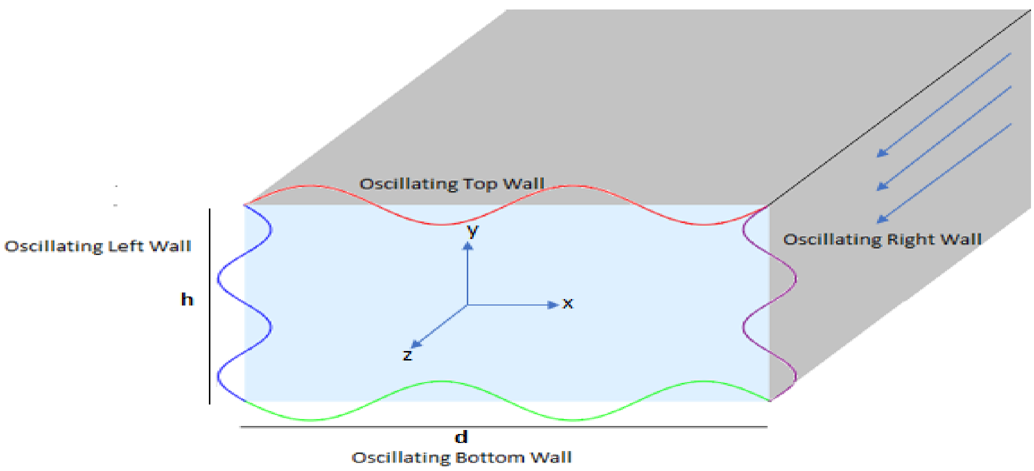

Fig. 1: Geometry of the problem.

The unsteady governing equations incorporating fractional derivatives in two dimensions along with the appropriate initial and boundary conditions, which are expressed as

$$\frac{\partial^\alpha w}{\partial t^\alpha} = \nu\left(1 + \frac{1}{\mu\theta_1\theta_2}\right)\left(\frac{\partial^2 w}{\partial x^2} + \frac{\partial^2 w}{\partial y^2}\right), \tag{6}$$

$$w(x,\ y,\ 0) = w_t(x,\ y,\ 0) = 0, \tag{6a}$$
$$w(0,\ y,\ t) = w(d,\ y,\ t) = w(x,\ 0,\ t) = w(x,\ h,\ t) = U_0 Cos\omega t. \tag{6b}$$

Where θ_1 and θ_2 are the material constants of Eyring-Powell fluid. α is the fractional calculus parameter such that $0 < \alpha < 1$.

Introducing the non-dimensional variables as follow

$$d = \frac{d^\star}{L}, w = \frac{w^\star}{U_0}, x = \frac{U_0}{\nu}x^\star, y = \frac{U_0}{\nu}y^\star, t = \frac{{U_0}^2}{\nu}t^\star, N = \frac{1}{\mu\theta_1\theta_2}, h = \frac{h^\star}{L}. \tag{7}$$

By substituting these non-dimensional variables in Eq. (6) to Eq. $(6b)$ and sitting aside the "⋆" symbols, we came back to the non-dimensional model with its respective equations and conditions

$$\frac{\partial^\alpha w}{\partial t^\alpha} = (1+N)\left(\frac{\partial^2 w}{\partial x^2} + \frac{\partial^2 w}{\partial y^2}\right), \tag{8}$$
$$w(x,y,0) = w_t(x,\ y,\ 0) = 0, \tag{8a}$$
$$w(0,y,t) = w(d,y,t) = w(x,0,t) = w(x,h,t) = Cos\omega t. \tag{8b}$$

4. Exact Solution

We will tackle the fractional differential equation described in Eq. (8) along with its initial and boundary conditions Eq. (8a) and Eq. (8b) by using a combination of techniques, namely the discrete Laplace transform, and double finite Fourier sine transform. To do this, we will multiply Eq. (8) by $\mathrm{Sin}(\alpha_m x)$ and $\mathrm{Sin}(\beta_n y)$, then integrate over the intervals $[0, d]\ \times\ [0, h]$ regarding x and y, while also considering Eq. (8b), we find that

$$\frac{\partial^\alpha w_{nm}(t)}{\partial t^\alpha} + (\alpha_m^2 + \beta_n^2)(1+N)w_{nm}(t) = (1+N)[1-(-1)^m][1-(-1)^n]\frac{\alpha_m^2+\beta_n^2}{\alpha_m\beta_n}Co \tag{9}$$

where $\alpha_m = \frac{m\pi}{d}$, $\beta_n = \frac{n\pi}{h}$, and

$$w_{mn}(t) = \int_0^d\int_0^h w(x,y,t)\, sin(\alpha_m x)\, sin(\beta_n y)\, dxdy, \quad m,n = 1,2,3\ ... \tag{10}$$

The double Fourier sine transform of $w(x,y,t)$ satisfy the initial conditions

$$w_{mn}(0) = \frac{\partial w_{mn}(0)}{\partial t} = 0. \tag{11}$$

By discrete Laplace transforms, Eq. (9) with initial conditions Eq. (11) can be expressed as

$$[q^\alpha + (\alpha_m^2+\beta_n^2)(1+N)]\bar{w}_{mn}(q) = [1-(-1)^m][1-(-1)^n]\left(\frac{\alpha_m^2+\beta_n^2}{\alpha_m\beta_n}\right)\left(\frac{q}{q^2+\omega^2}\right),$$

which can be simplified as

$$\bar{w}_{mn}(q) = \varphi_{mn}\cdot\frac{q}{q^2+\omega^2} - \varphi_{mn}\left(\frac{q}{q^2+\omega^2}\right)\cdot\frac{q^\alpha}{q^\alpha+\chi_{mn}(1+N)}, \tag{12}$$

Where

$$\varphi_{mn} = \frac{1}{\alpha_m\beta_n}[1-(-1)^m][1-(-1)^n], \qquad \chi_{mn} = \alpha_m^2+\beta_n^2, \tag{13}$$

and

$\bar{w}_{mn}(q) = \int_0^\infty w_{mn}(t)e^{-qt}dt,$ is the Laplace transform of $w_{mn}(t)$.

We consider the function

$$G_{mn}(q) = \frac{q^\alpha}{q^\alpha+\chi_{mn}(1+N)},$$

we can also write it as

$$G_{mn}(q) = \frac{1}{1 + \frac{\chi_{mn}(1+N)}{q^{\alpha}}} = \sum_{k=1}^{\infty} (-\chi_{mn})^k \cdot \frac{(1+N)^k}{q^{\alpha k}}. \tag{14}$$

Now Eq. (10) become as

$$\bar{w}_{mn}(q) = \varphi_{mn} \cdot \frac{q}{q^2+\omega^2} - \varphi_{mn}\left(\frac{q}{q^2+\omega^2}\right) G_{mn}(q). \tag{15}$$

By applying the double inverse Fourier sine transform to Eq. (15), we get the following

$$\bar{w} = \frac{4}{dh} \cdot \frac{q}{q^2+\omega^2} \sum_{m=1}^{\infty}\sum_{n=1}^{\infty} \varphi_{mn} \sin(\alpha_m x)\sin(\beta_n y) - \frac{4}{dh} \cdot \sum_{m=1}^{\infty}\sum_{n=1}^{\infty} \varphi_{mn} \sin(\alpha_m x)\sin(\beta_n y)\left(\frac{q}{q^2+\omega^2}\right) G_{mn}(q). \tag{16}$$

After simplification, we obtain the expression

$$\bar{w} = \frac{q}{q^2+\omega^2} - \frac{4}{dh} \cdot \sum_{m=1}^{\infty}\sum_{n=1}^{\infty} \varphi_{mn} Sin(\alpha_m x) Sin(\beta_n y)\left(\frac{q}{q^2+\omega^2}\right) G_{mn}(q). \tag{17}$$

With the help of inverse Laplace transform to Eq. (17) we get this expression

$$w = Cos\omega t - \frac{4}{dh} \cdot \sum_{m=1}^{\infty}\sum_{n=1}^{\infty} \varphi_{mn} Sin(\alpha_m x) Sin(\beta_n y) \sum_{k=1}^{\infty} ((-\chi_{mn})(1+N))^k \cdot \left(Cos\omega t * \frac{t^{\alpha k-1}}{\Gamma(\alpha k)}\right). \tag{18}$$

Now, sitting d=2a, d=2b, and using the convolution operator (∗), Eq. (18) become as

$$w = Cos\omega t - \frac{1}{ab} \cdot \sum_{m=1}^{\infty}\sum_{n=1}^{\infty} \varphi_{mn} Sin(\alpha_m x) Sin(\beta_n y) \sum_{k=1}^{\infty} ((-\chi_{mn})(1+N))^k \cdot \int_0^t Cos\omega(t-\xi).\,\xi^{\alpha k-1}\, d\xi. \tag{19}$$

Using the widely recognized mathematical software "Mathematica", we can write

$$w = Cos\omega t - \frac{1}{ab} \cdot \sum_{m=1}^{\infty}\sum_{n=1}^{\infty} \varphi_{mn} Sin(\alpha_m x) Sin(\beta_n y) \sum_{k=1}^{\infty} ((-\chi_{mn})(1+N))^k \times t^{k\alpha}\left(\frac{Cos[t\omega] HypergeometricPFQ\left[\left\{\frac{k\alpha}{2}\right\},\left\{\frac{1}{2}, 1+\frac{k\alpha}{2}\right\}, -\frac{1}{4}t^2\omega^2\right]}{k\alpha} + \frac{t\omega HypergeometricPFQ\left[\left\{\frac{1}{2}+\frac{k\alpha}{2}\right\},\left\{\frac{3}{2}, \frac{3}{2}+\frac{k\alpha}{2}\right\}, -\frac{1}{4}t^2\omega^2\right] Sin[\omega t]}{1+k\alpha}\right) \tag{20}$$

The exact solution of fractionalized NTNN fluid in a rectangular duct is presented in Eq. (20). There are some special cases of Eq. (20), which are given as

Special case I:

If $\alpha = 1$,we can get similar analytical solution of velocity field for ordinary NTNN model. Consequently, the field of velocity reduces to

$$w = Cos\omega t - \frac{1}{ab} \cdot \sum_{m=1}^{\infty}\sum_{n=1}^{\infty} \varphi_{mn}\, Sin(\alpha_m x)\, Sin(\beta_n y) \sum_{k=1}^{\infty} ((-\chi_{mn})(1+N))^k \cdot t^k \left(\frac{Cos[t\omega] HypergeometricPFQ\left[\left\{\frac{k}{2}\right\}, \left\{\frac{1}{2}, 1+\frac{k}{2}\right\}, -\frac{1}{4}t^2\omega^2\right]}{k} + \frac{t\omega HypergeometricPFQ\left[\left\{\frac{1}{2}+\frac{k}{2}\right\}, \left\{\frac{3}{2}, \frac{3}{2}+\frac{k}{2}\right\}, -\frac{1}{4}t^2\omega^2\right] Sin[t\omega]}{1+k} \right) \tag{21}$$

Special case II:

If $N = 0$, we can get analogous exact solution of velocity field for Newtonian fluid. Consequently, the field of velocity reduces to

$$w = Cos\omega t - \frac{1}{ab} \cdot \sum_{m=1}^{\infty}\sum_{n=1}^{\infty} \varphi_{mn}\, Sin(\alpha_m x)\, Sin(\beta_n y) \sum_{k=1}^{\infty} (-\chi_{mn})^k \cdot t^{k\alpha} \left(\frac{Cos[t\omega] HypergeometricPFQ\left[\left\{\frac{k\alpha}{2}\right\}, \left\{\frac{1}{2}, 1+\frac{k\alpha}{2}\right\}, -\frac{1}{4}t^2\omega^2\right]}{k\alpha} + \frac{t\omega HypergeometricPFQ\left[\left\{\frac{1}{2}+\frac{k\alpha}{2}\right\}, \left\{\frac{3}{2}, \frac{3}{2}+\frac{k\alpha}{2}\right\}, -\frac{1}{4}t^2\omega^2\right] Sin[\omega t]}{1+k\alpha} \right) \tag{22}$$

5. Calculation of Shear Stresses

Shear stress tensors for this problem are

$$\boldsymbol{\tau_1} = \mu(1+N)\frac{\partial w}{\partial x}, \tag{23}$$

$$\boldsymbol{\tau_2} = \mu(1+N)\frac{\partial w}{\partial y} \tag{24}$$

Now, we denote τ_1, τ_2 by τ_{1c}, τ_{2c} (tensions for cosine oscillation of duct).
If we bring in

$$T_1 = \tau_{1c}, \quad T_2 = \tau_{2c}, \tag{25}$$

we obtain

$$T_1 = \mu(1+N)\frac{\partial w}{\partial x}, \tag{26}$$

$$T_2 = \mu(1+N)\frac{\partial w}{\partial y}. \tag{27}$$

And initial conditions are

$$T_1(x,y,0) = T_2(x,y,0) = 0. \tag{28}$$

Apply the Laplace transforms on Eq. (26) and Eq. (27) alongside initial conditions Eq. (28), we get the following

$$\bar{T}_1 = \mu(1+N)\frac{\partial \bar{w}}{\partial x}, \tag{29}$$

$$\bar{T}_2 = \mu(1+N)\frac{\partial \bar{w}}{\partial y}. \tag{30}$$

Now use Eq. (17) into Eq. (29) and Eq. (30) with d=2a and h=2b, we have

$$\bar{T}_1=-\frac{\mu(1+N)}{ab}\cdot\sum_{m=1}^{\infty}\sum_{n=1}^{\infty}\varphi_{mn}\frac{Cos(\alpha_m x)}{\alpha_m}Sin(\beta_n y)\left(\frac{q}{q^2+\omega^2}\right)G_{mn}(q), \tag{31}$$

$$\bar{T}_2=-\frac{\mu(1+N)}{ab}\cdot\sum_{m=1}^{\infty}\sum_{n=1}^{\infty}\varphi_{mn}Sin(\alpha_m x)\frac{Cos(\beta_n y)}{\beta_n}\left(\frac{q}{q^2+\omega^2}\right)G_{mn}(q). \tag{32}$$

Applying inverse Laplace transform to Eq. (31) and Eq. (32), and employing widely recognized mathematical software "Mathematica", we obtain the following expression

$$\tau_1=-\frac{\mu}{ab}\sum_{m=1}^{\infty}\sum_{n=1}^{\infty}\varphi_{mn}\frac{Cos(\alpha_m x)}{\alpha_m}Sin(\beta_n y)\sum_{k=1}^{\infty}(-\chi_{mn})^k\cdot(1+N)^{k+1}$$
$$\cdot t^{k\alpha}\left(\frac{Cos[t\omega]HypergeometricPFQ\left[\left\{\frac{k\alpha}{2}\right\},\left\{\frac{1}{2},1+\frac{k\alpha}{2}\right\},-\frac{1}{4}t^2\omega^2\right]}{k\alpha}+\frac{t\omega HypergeometricPFQ\left[\left\{\frac{1}{2}+\frac{k\alpha}{2}\right\},\left\{\frac{3}{2},\frac{3}{2}+\frac{k\alpha}{2}\right\},-\frac{1}{4}t^2\omega^2\right]Sin[\omega t]}{1+k\alpha}\right) \tag{33}$$

$$\tau_2=-\frac{\mu}{ab}\sum_{m=1}^{\infty}\sum_{n=1}^{\infty}\varphi_{mn}Sin(\alpha_m x)\frac{Cos(\beta_n y)}{\beta_n}\sum_{k=1}^{\infty}(-\chi_{mn})^k\cdot(1+N)^{k+1}$$
$$\cdot t^{k\alpha}\left(\frac{Cos[t\omega]HypergeometricPFQ\left[\left\{\frac{k\alpha}{2}\right\},\left\{\frac{1}{2},1+\frac{k\alpha}{2}\right\},-\frac{1}{4}t^2\omega^2\right]}{k\alpha}+\frac{t\omega HypergeometricPFQ\left[\left\{\frac{1}{2}+\frac{k\alpha}{2}\right\},\left\{\frac{3}{2},\frac{3}{2}+\frac{k\alpha}{2}\right\},-\frac{1}{4}t^2\omega^2\right]Sin[\omega t]}{1+k\alpha}\right). \tag{34}$$

6. Findings and discussion

In this article, we have investigated the flow properties of fractional NTNN fluid within a rectangular duct subject to oscillation. By employing the double finite Fourier sine transform and discrete Laplace transform, we obtained solution for cosine oscillations that converge to those of both conventional NTNN and Newtonian fluids under specific circumstances. To sum up, we have visually represented the impact of different variables on velocity field characteristics through graphical displays. By adjusting non-dimensional parameters like the non-integer fractional parameter α, fluid parameter N, and angular velocity ω, we have demonstrated their effects on the velocity field, offering a thorough comprehension of fluid flow behavior. In Figure 2, it's evident that the fluid velocity field expands as the accelerating non-integer fractional parameter α values increase. In Figure 3, we observe that the velocity field accelerates as the fluid parameter N increases. Figure 4 depicts how the profile of velocity for cosine oscillation is affected by oscillation frequency, denoted as ω. As the values of ω rise, the velocity experiences a corresponding increase. This occurs because a higher angular frequency implies that an object undergoes more oscillations or rotations per unit time, leading to a greater linear velocity. Figure 5 depicts the fluctuations in the velocity profile across various time values. The graphic reveals a direct proportionality between the impact of time and the transient velocity concerning the spatial coordinate y. Figures. 6-9 examine the shear stresses corresponding to the non-integer fractional parameter α and fluid parameter N. The shear stresses have the same behavior for these parameters as velocity field. Figure 10 is set up to analyze how the velocity field behaves for Eq. (18) and Eq. (19) as the fractional parameter α varies. It's observed that the velocity magnitude of conventional NTNN is higher than that of Fractional NTNN. In Figure 11, when we compare Eq. (18) and Eq. (20), we see that the fractional NTNN fluid has a higher velocity than the Newtonian fluid.

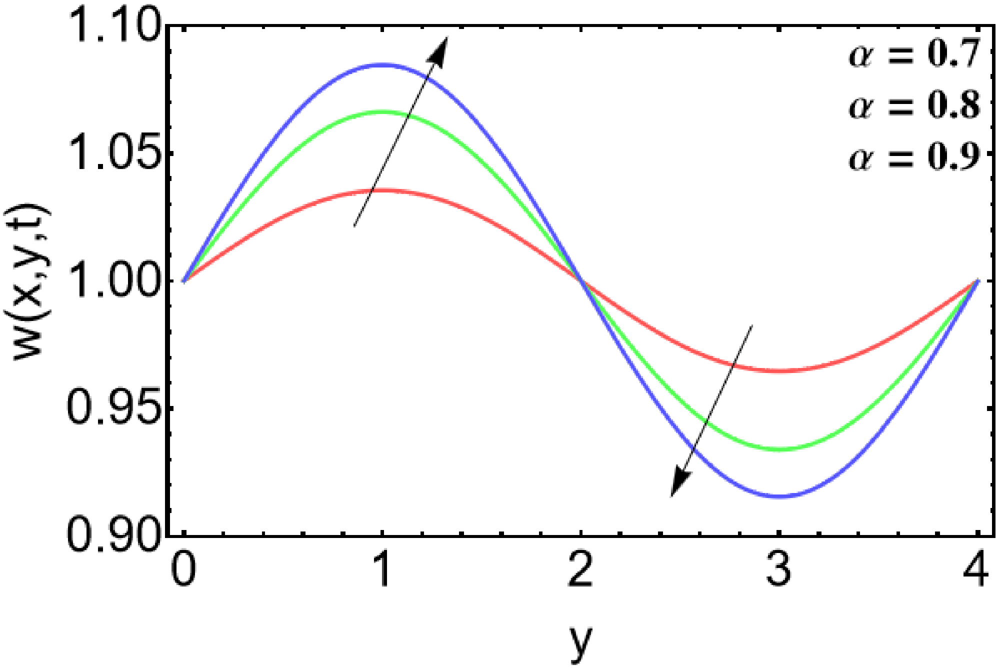

Fig. 2: Velocity profile corresponding to α with $x = 0.01, a = 2, b = 1, t = 2, \omega = 2\pi, N = 0.7$.

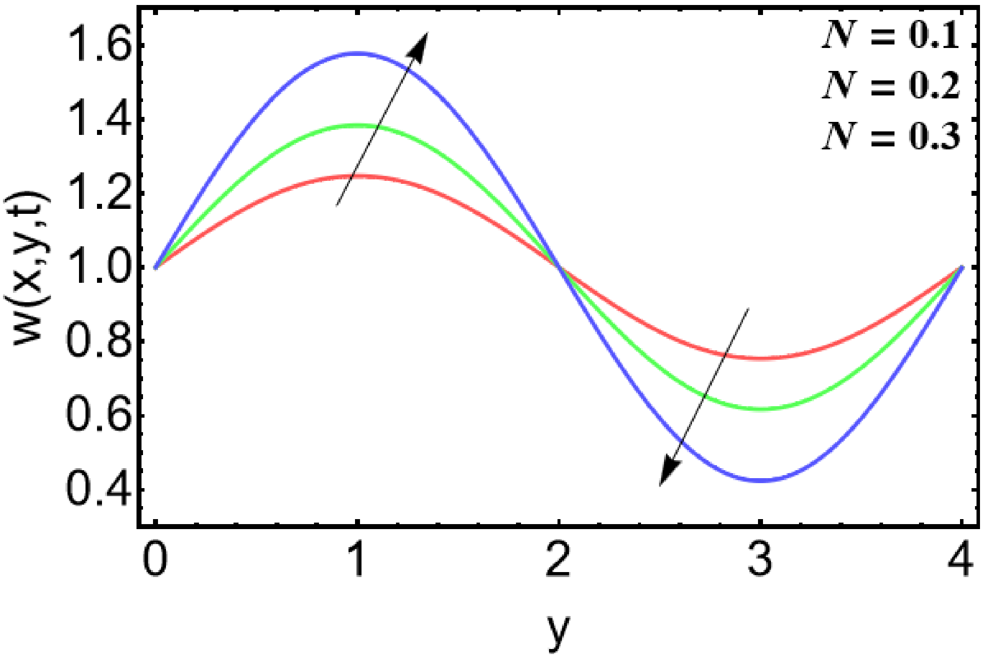

Fig. 3: Velocity field corresponding to N with $x = 0.01, a = 2, b = 1, t = 2, \alpha = 0.6, \omega = 2\pi$.

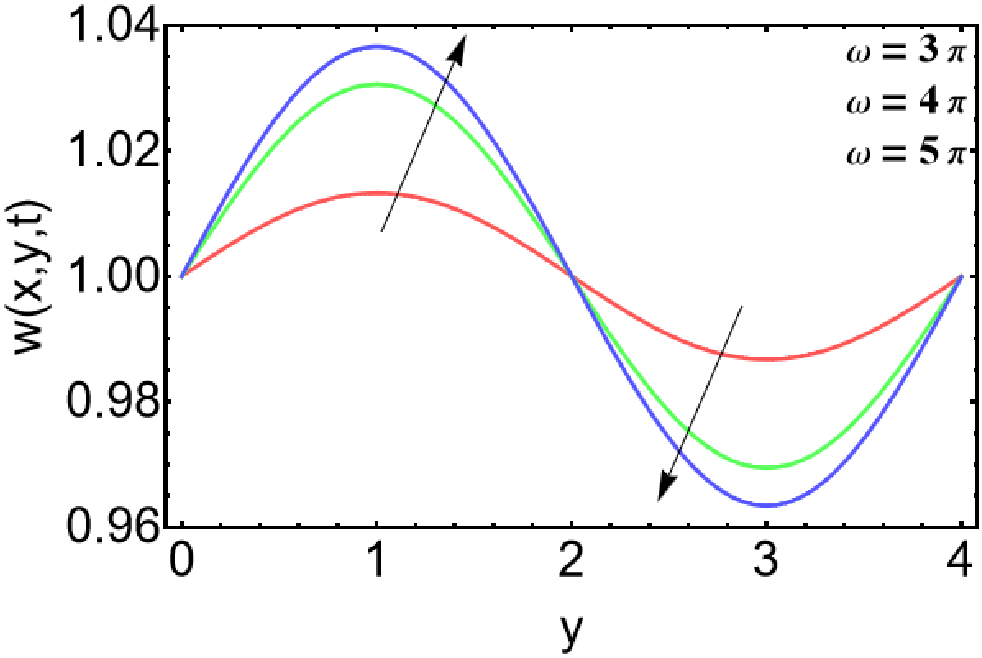

Fig. 4: Velocity field corresponding to ω with $x = 0.01, a = 2, b = 1, t = 2, \alpha = 0.6, N = 0.7$.

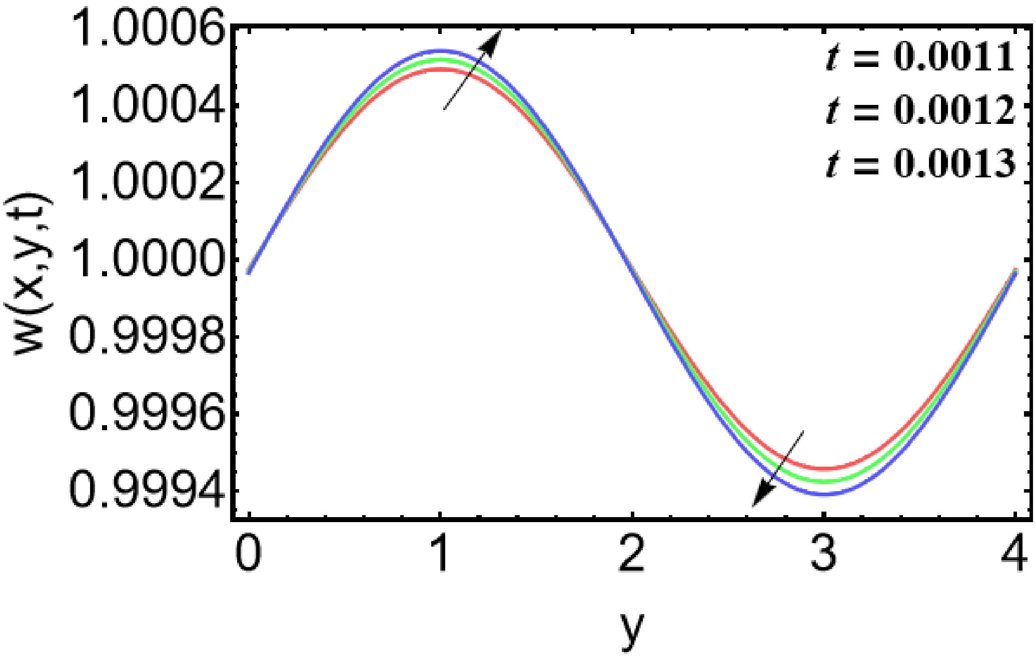

Fig. 5: Velocity field corresponding to t with $x = 0.01, a = 2, b = 1, \alpha = 0.6, \omega = 2\pi, N = 0.7$.

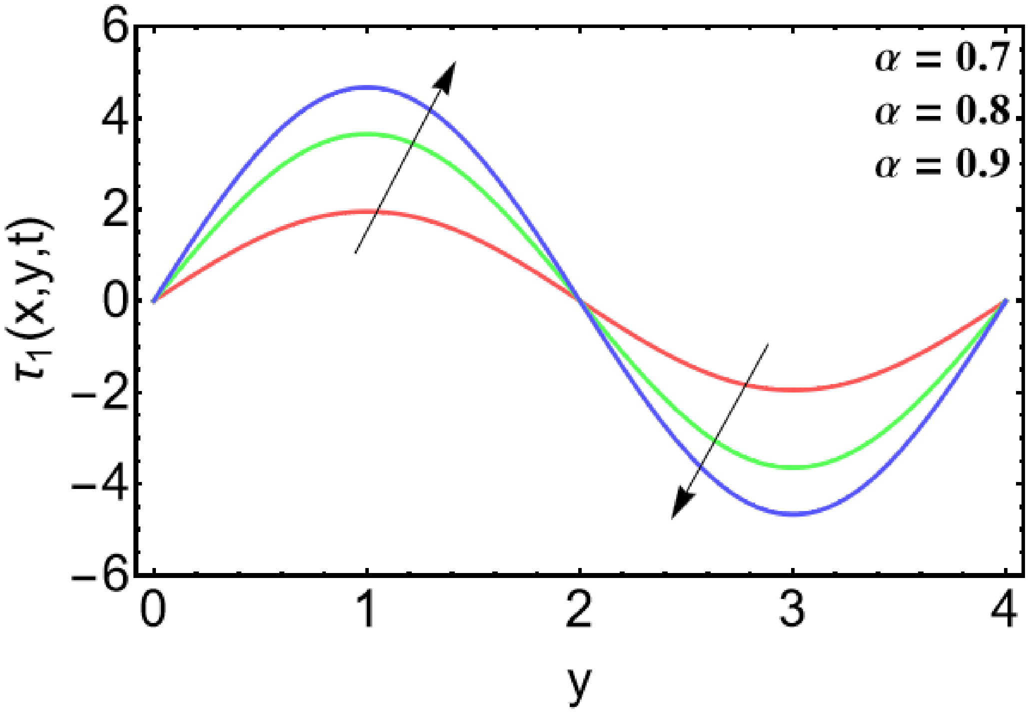

Fig. 6: Shear stresses corresponding to α with $x = 0.01, a = 2.0, b = 1.0, t = 2, \omega = 2\pi, N = 0.7,$ $\mu = 0.2.$

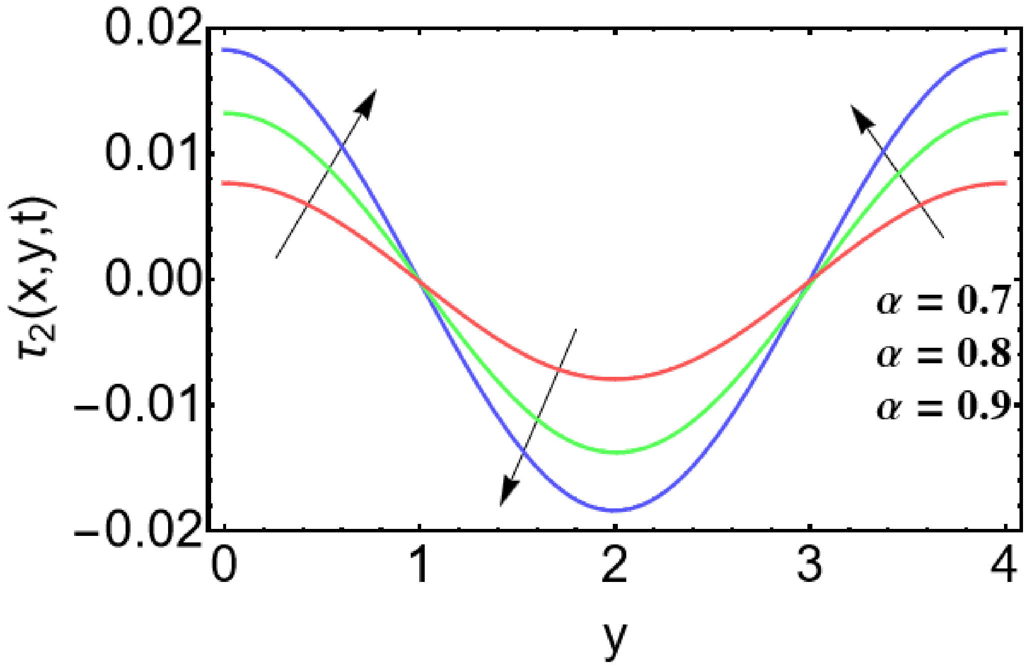

Fig. 7: Shear stresses corresponding to α with $x = 0.01, a = 2.0, b = 1.0, t = 2, \omega = 2\pi, N = 0.7,$ $\mu = 0.2.$

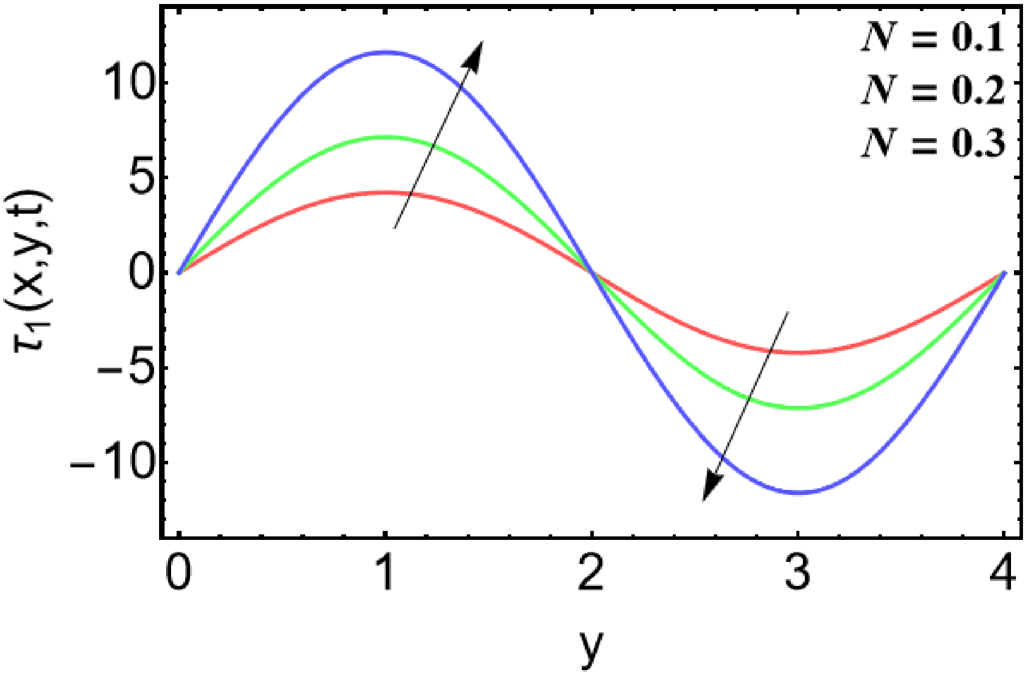

Fig. 8: Shear stresses corresponding to N with $x = 0.01, a = 2.0, b = 1.0, t = 2, \alpha = 0.6, \omega = 2\pi,$ $\mu = 0.2.$

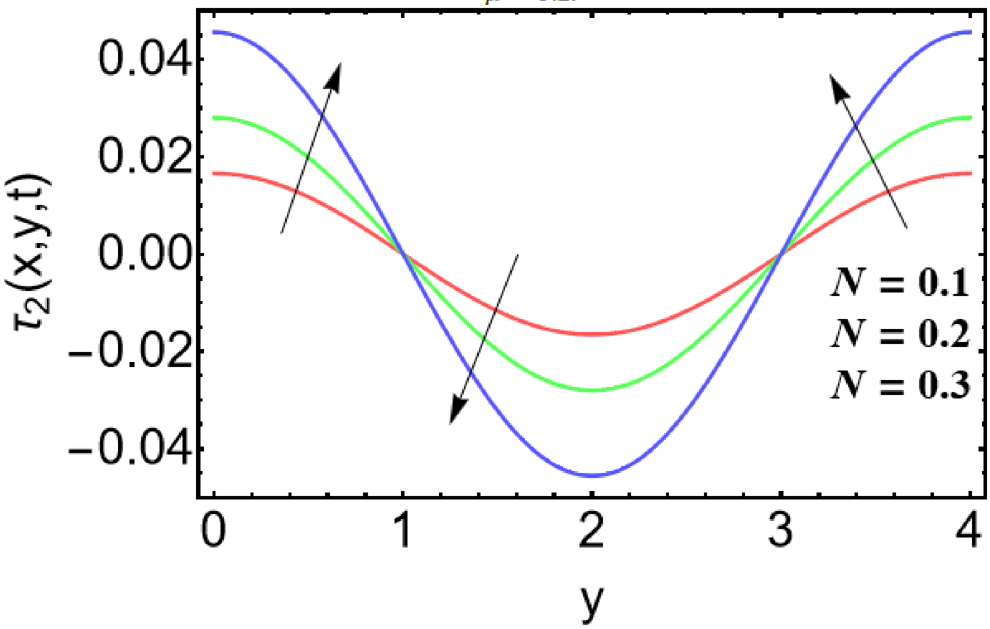

Fig. 9: Shear stresses corresponding to N with $x = 0.01, a = 2.0, b = 1.0, t = 2, \alpha = 0.6, \omega = 2\pi,$ $\mu = 0.2.$

7. Concluding remarks

The exact solution is obtained in this chapter by using double finite Fourier sine transform and discrete Laplace transforms for field of velocity and associated with it shear stresses corresponding to the unsteady flow of Fractional NTNN fluids through an oscillating duct of rectangular cross-section. The finding shows that the solutions of ordinary NTNN fluid and Newtonian fluid, performing similar flow behavior, appear as the limiting cases of the obtained solution. This study discovers the consequences of various rheological parameters including $\alpha, N, \omega,$ and t on the motion of the fractional NTNN fluid. The key findings and recommendations arising from this investigation include

- Fluid flow velocity exhibits an increasing trend with rising values of parameters α and N.
- Fluid flow velocity rises with increasing values of ω and t.
- The behavior of fluid flow shear stress closely parallels that of fluid flow velocity concerning parameters α and N.

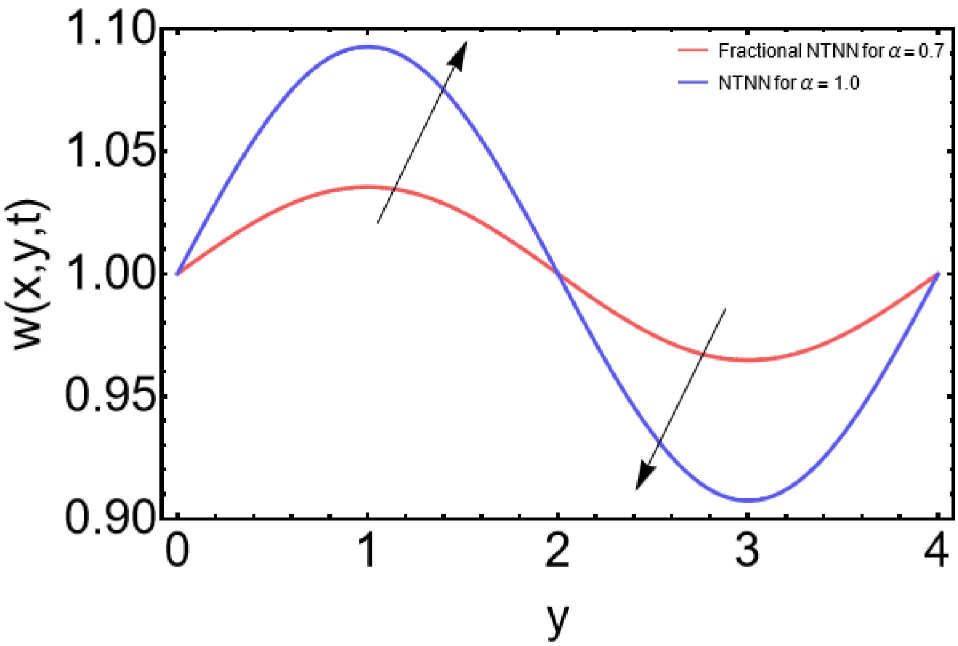

Fig. 10: Velocity profile corresponding to α with $x = 0.01, a = 2, b = 1, t = 2, \omega = 2\pi, N = 0.7$.

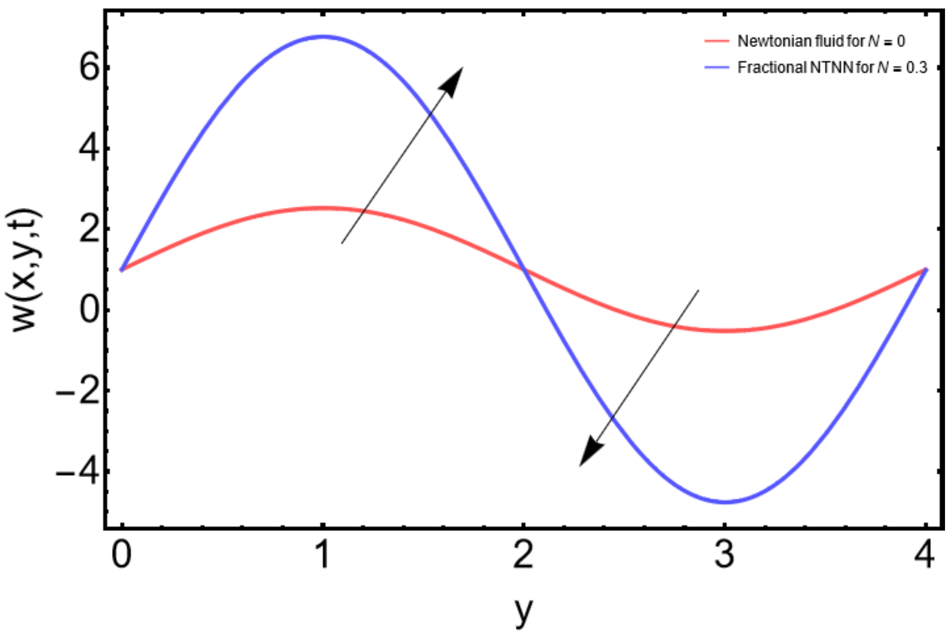

Fig. 11: Velocity profile corresponding to N with $x = 0.01, a = 2, b = 1, t = 2, \alpha = 0.6, \omega = 2\pi$.

Acknowledgement

Authos S. Nadeem and J. Alzabut are thankful to Prince Sultan university for the support

References

[1] M. Abu-Shady, M. K. A. Kaabar, A Generalized Definition of the Fractional Derivative with Applications, *Mathematical Problems in Engineering,* Vol. 2021, No. 1, pp. 9444803, 2021.

[2] A. Raza, T. Thumma, S. U. Khan, M. Boujelbene, A. Boudjemline, I. A. Chaudhry, I. Elbadawi, Thermal mechanism of carbon nanotubes with Newtonian heating and slip effects: A Prabhakar fractional model, *Journal of the Indian Chemical Society*, Vol. 99, No. 10, pp. 100731, 2022/10/01/, 2022.

[3] T. Anwar, P. Kumam, Asifa, P. Thounthong, S. Muhammad, F. Z. Duraihem, Generalized thermal investigation of unsteady MHD flow of Oldroyd-B fluid with slip effects and Newtonian heating; a Caputo-Fabrizio fractional model, *Alexandria Engineering Journal,* Vol. 61, No. 3, pp. 2188-2202, 2022/03/01/, 2022.

[4] E. Viera-Martin, J. F. Gómez-Aguilar, J. E. Solís-Pérez, J. A. Hernández-Pérez, R. F. Escobar-Jiménez, Artificial neural networks: a practical review of applications involving fractional calculus, *The European Physical Journal Special Topics,* Vol. 231, No. 10, pp. 2059-2095, 2022/08/01, 2022.

[5] N. A. Sheikh, D. L. C. Ching, I. Khan, D. Kumar, K. S. Nisar, A new model of fractional Casson fluid based on generalized Fick's and Fourier's laws together with heat and mass transfer, *Alexandria Engineering Journal*, Vol. 59, No. 5, pp. 2865-2876, 2020/10/01/, 2020.

[6] N. Sene, Analytical Solutions of a Class of Fluids Models with the Caputo Fractional Derivative, *Fractal and Fractional,* Vol. 6, No. 1, pp. 35, 2022.

[7] S. Nadeem, B. Ishtiaq, J. Alzabut, S. M. Eldin, Three parametric Prabhakar fractional derivative-based thermal analysis of Brinkman hybrid nanofluid flow over exponentially heated plate, *Case Studies in Thermal Engineering,* Vol. 47, pp. 103077, 2023/07/01/, 2023.

[8] A. Rauf, A. Muhammad, Multi-layer flows of immiscible fractional second grade fluids in a rectangular channel, *SN Applied Sciences*, Vol. 2, No. 10, pp. 1714, 2020/09/21, 2020.

[9] S. Nadeem, B. Ishtiaq, J. Alzabut, A. M. Hassan, Fractional Nadeem trigonometric non-Newtonian (NTNN) fluid model based on Caputo-Fabrizio fractional derivative with heated boundaries, *Scientific Reports,* Vol. 13, No. 1, pp. 21511, 2023/12/06, 2023.

[10] I. Barmak, D. Picchi, A. Gelfgat, N. Brauner, Flow of a shear-thinning fluid in a rectangular duct, *Physical Review Fluids,* Vol. 9, No. 2, pp. 023303, 02/13/, 2024.

[11] S. Nadeem, B. Ishtiaq, J. Alzabut, S. M. Eldin, Implementation of differential transform method on the squeezing flow of trigonometric non-Newtonian fluid between two heated plates, *International Journal of Modern Physics B,* Vol. 38, No. 24, pp. 2450326, 2024.

[12] M. Ghalib, A. Zafar, Z. Hammouch, M. Riaz, K. Shabbir, Analytical results on the unsteady rotational flow of fractional-order non-Newtonian fluids with shear stress on the boundary, *Discrete and Continuous Dynamical Systems - Series S,* Vol. 13, 11/21, 2018.

[13] H. Zahir, Mehnaz, J. Gul, M. Inc, R. T. Alqahtani, Impact of fractional magnetohydrodynamic and hall current on ree-eyring fluid flow by using radial basis function method, *Alexandria Engineering Journal,* Vol. 88, pp. 210-215, 2024/02/01/, 2024.

[14] M. Arif, P. Kumam, W. Watthayu, Analysis of constant proportional Caputo operator on the unsteady Oldroyd-B fluid flow with Newtonian heating and non-uniform temperature, *ZAMM - Journal of Applied Mathematics and Mechanics / Zeitschrift für Angewandte Mathematik und Mechanik,* Vol. 104, No. 2, pp. e202300048, 2024.

[15] A. Al Agha, Z. A. M., R. Muhammad, S. Ahmad, A. Shajar, N. Mudassar, H. and Al Garalleh, Analysis of active and passive control of fluid with fractional derivative, *Numerical Heat Transfer, Part A: Applications*, pp. 1-19.

[16] S. Sarwar, M. Aleem, M. A. Imran, A. Akgül, A comparative study on non-Newtonian fractional-order Brinkman type fluid with two different kernels, *Numerical Methods for Partial Differential Equations,* Vol. 40, No. 1, pp. e22688, 2024.